*J. Plasma Physics* (2004), *vol.* 70, *part* 2, *pp.* 185–197. © 2004 Cambridge University Press 
DOI: 10.1017/S0022377803002538 Printed in the United Kingdom

# Classical bremsstrahlung in a non-ideal plasma with effective interaction

A. WIERLING[1], Th. MILLAT[2] and G. RÖPKE[2]

[1]Department of Fundamental Energy Science, Kyoto University, Uji, Kyoto, 611-0011, Japan
[2]Fachbereich Physik, Universität Rostock, 18051 Rostock, Germany
(wierling@center.iae.kyoto-u.ac.jp)

(Received 1 July 2003 and in revised form 30 October 2003)

**Abstract.** The emission coefficient due to classical electron–ion bremsstrahlung is calculated for a non-ideal plasma with an effective interaction. An approach due to Gould is used to obtain the emission coefficient for bremsstrahlung. It is shown that this result can also be derived from an approximation to the force–force correlation function assuming no correlations among particles. The trajectory for electrons in the effective potential is determined by the numerical solution of Newton's equation. Comparison is made with molecular dynamics results for the dynamical collision frequency.

## 1. Introduction

Electron–ion bremsstrahlung is the most important emission process in fully ionized, isotropic plasmas. Even in partially ionized plasmas, bremsstrahlung contributes to the continuum spectrum. Bremsstrahlung emission can be used to infer plasma parameters such as the density and temperature in a plasma (Griem 1997; Hutchinson 1987). Furthermore, details about the one-particle distribution function can be gathered (Voss and Fisch 1992).

A number of approximations have been cultivated to determine the bremsstrahlung spectrum for ideal plasmas (Bekefi 1966; Sobelman 1992; Jackson 1999). In non-ideal plasmas, correlation effects have to be accounted for. These corrections range from dynamical screening (Dawson and Oberman 1962), local field corrections (Berkovsky and Kurilenkov 1993), ionic structure (Cauble and Rozmus 1985), degeneracy (Kawakami et al. 1988) to nonlinear effects (Silin 1965; Decker et al. 1994; Bornath et al. 2001) depending on the plasma conditions. In Wierling et al. (2001), we proposed a quantum-statistical approach to obtain a systematic perturbative treatment of many-body effects for the emission spectrum. We compared our results to molecular dynamics (MD) simulation studies of the electron–ion collision frequency in a non-ideal plasma (Pfalzner and Gibbon 1998). However, the simulation was carried out by solving the classical equation of motion for the electrons using an effective potential. Thus, a direct comparison of our theoretical approach with simulation results is biased.

It has been noted by several authors, that a classical treatment of bremsstrahlung leads to reasonable approximations for the quantum-mechanical expressions in many cases. A very successful approach to the cross section of classical

https://doi.org/10.1017/S0022377803002538 Published online by Cambridge University Press

bremsstrahlung is due to Gould (1970) and has been applied to a variety of plasma conditions recently (Jung 1994, 2002; Jung and Jeong 1996). Carrying out this approach, different approximative methods to describe the classical motion of particles in a plasma have been studied, such as the straight-line (SL) and the hyperbolic-orbit (HO) trajectory methods. In addition, the numerical solution for the classical bremsstrahlung cross section has been advanced (Kim et al. 1987).

The objective of this paper is to calculate the emission coefficient for bremsstrahlung radiation for the effective potential used in the simulation and to compare it with the simulation results for the collision frequency. To be consistent with the simulation, no quantum-mechanical arguments are used. In this context, a comparison between the different approximative solutions for the expression proposed by Gould is given. Furthermore, since the simulation is carried out in the weakly nonlinear regime for the external electro-magnetic field, an extrapolation scheme to the linear domain is presented.

The paper is organized as follows. In Sec. 2, we review the approach due to Gould and introduce possible approximations. In Sec. 3, the molecular dynamics simulation is described and the extrapolation scheme is explained in detail. A comparison between the simulation and theoretical results is given in Sec. 4. The findings are summarized and improvements are suggested in Sec. 5. In Appendix A, the approach of Gould is reproduced by calculating the force–force correlation function in an impurity scattering model assuming no correlations among particles.

## 2. Classical approach to bremsstrahlung

In the classical approach to bremsstrahlung (Bekefi 1966; Gould 1970; Landau and Lifshitz 1995), the emission coefficient for radiation $j_\omega$ can be obtained from the emission power $dW/d\omega\, dt$ per $4\pi$ and frequency by thermal averaging

$$j_\omega = n_\mathrm{e} n_\mathrm{i} \left(\frac{m}{2\pi k_\mathrm{B} T}\right)^{3/2} \int_{v_\mathrm{min}}^{\infty} dv\, v^3 e^{-mv^2/(2k_\mathrm{B}T)} 2\pi \int_0^\infty db\, b \frac{dW}{d\omega\, dt}, \tag{2.1}$$

where the cut-off velocity is given as $v_\mathrm{min} = (2\hbar\omega/m)^{1/2}$. The emitted power is determined using Larmor's formula,

$$\frac{dW}{d\omega\, dt} = \frac{2e^2}{3\epsilon_0 m^2 c^3} |\vec{F}_\omega|^2. \tag{2.2}$$

Here, $\vec{F}_\omega$ is the Fourier coefficient of the force acting on the electron moving along a trajectory given by $\vec{r}(t)$,

$$\vec{F}_\omega = \frac{1}{2\pi} \int_{-\infty}^{\infty} dt e^{i\omega t} \vec{F}(\vec{r}(t)). \tag{2.3}$$

The assumption is made that electrons collide with ions which are at rest and randomly distributed. $n_\mathrm{e}$ is the electron density, $n_\mathrm{i}$ is the ion density and $m$ is the reduced mass of the electrons. Any correlations among the electrons or ions are neglected in this formula. In the classical limit, $\hbar\omega \ll k_\mathrm{B}T$, the cut-off velocity can be approximated by $v_\mathrm{min} = 0$. Taking the electron trajectory in the $(x, y)$ plane, we have $|\vec{F}_\omega|^2 = |F_{x\omega}|^2 + |F_{y\omega}|^2$.

https://doi.org/10.1017/S0022377803002538 Published online by Cambridge University Press

In a plasma, the force acting on an electron is not given by the Coulomb interaction, but is modified due to many-body correlations. In particular, screening corrections are important for plasmas at moderate coupling. This leads to a dynamical screened potential $V^{\mathrm{s}}$ given by, (see (Kraeft et al. 1986)),

$$V^{\mathrm{s}}(q,\omega) = V(q)/\epsilon(q,\omega), \tag{2.4}$$

where the screening is provided by the dielectric function $\epsilon(q,\omega)$. The quantum mechanical treatment (Wierling et al. 2001) has shown that effects due to dynamical screening are small, apart from a region close to the plasma frequency, and the overall frequency-dependence of the dynamical collision frequency can be well described by static screening $\epsilon(q,\omega) \approx \epsilon(q,0)$. This is also noted in the classical treatment of Dawson and Oberman (1962). Thus, we assume static screening leading to a Debye–Hückel-like effective potential.

In a real plasma, the stability of the electron–ion system is guaranteed by quantum-mechanics. In classical simulations, however, the stability has to be imposed. For example, an effective soft-core potential is used to avoid Coulomb implosion. There are a number of different choices in the literature, in particular potentials which are obtained from quantum statistical approaches such as the Kelbg (1963) and the Deutsch potential (Deutsch 1977). In Pfalzner and Gibbon (1998), a soft-core potential of the form

$$V(r) = -\frac{e^2}{4\pi\epsilon_0}\frac{1}{(r^2+\epsilon^2)^{1/2}} \tag{2.5}$$

was used, where $\epsilon$ is a parameter chosen in the simulation. Including screening effects, the effective potential used in this paper is taken to be

$$V^{\mathrm{s,e}}(r) = -\frac{e^2}{4\pi\epsilon_0}\frac{1}{(r^2+\epsilon^2)^{1/2}}e^{-\kappa r}. \tag{2.6}$$

Here, $\kappa$ denotes the inverse screening length. The corresponding force is given by

$$\vec{F}^{\mathrm{s,e}}(r) = \frac{e^2}{4\pi\epsilon_0}\frac{e^{-\kappa r}}{(r^2+\epsilon^2)^{3/2}}\left(1+\kappa\frac{r^2+\epsilon^2}{r}\right)\vec{r}. \tag{2.7}$$

Note, that in a textbook treatment (cf. Jackson (1999)), the cut-offs $b_{\min}$ and $b_{\max}$ are introduced for the integration over the impact parameter in (2.1). The minimal value $b_{\min}$ is introduced to take care of quantum-mechanical effects as well as effects due to strong collisions, while the maximum value $b_{\max}$ establishes screening. However, screening is included in our effective potential. Furthermore, the existence of strong collisions is already accounted for by solving the equation of motion numerically. Thus, there is no need to introduce these cut-offs within our approach.

To determine the Fourier coefficient (2.3), different approximative and exact methods have been advanced. The simplest approach is the straight line approximation (Jackson 1999; Gould 1970; Jung 1996), where the trajectory is approximated by an uniform motion along the $x$-axis given as

$$x(t) = vt; \quad y(t) = b. \tag{2.8}$$

A more refined description of the trajectory is given by the HO trajectory method (Landau and Lifshitz 1995; Jung and Jeong 1996). A convenient parametric

https://doi.org/10.1017/S0022377803002538 Published online by Cambridge University Press

representation is given by

$$x = d(f^2 - 1)^{1/2} \sinh w, \tag{2.9}$$

$$y = d(f - \cosh w), \tag{2.10}$$

$$r(t) = d(f \cosh w - 1), \tag{2.11}$$

$$t = \frac{d}{v}(e \sinh w - w). \tag{2.12}$$

Here, $d$ is half the distance of the closest approach in a head-on collision, $f$ is the eccentricity, $v$ is the initial velocity of the projectile and $-\infty < w < \infty$. The distance $d$ has to be calculated for the effective force $\vec{F}^{\mathrm{s,e}}$.

Finally, an exact determination is possible by solving the differential equation for motion in a central field given by the force $\vec{F}^{\mathrm{s,e}}$. We follow Kim and Pratt (1987) and change to a coordinate system, where the trajectory is symmetric to one of the coordinate axes. Such a coordinate system can be obtained by rotation from the original. Since $|\vec{F}_\omega|^2$ is invariant under rotation, it can be determined in the rotated coordinate system. Parameterizing the trajectory by polar coordinates, the radial differential equation reads

$$\dot{r} = \sqrt{\frac{2}{m}}\left(T - V(r) - \frac{L^2}{2mT^2}\right)^{1/2}, \tag{2.13}$$

where $T = mv^2/2$ is the kinetic energy and $L$ is the angular momentum, which is fixed by the impact parameter $L^2 = 2mTb^2$. The angular differential equation states

$$mbv = mr^2\dot{\phi}. \tag{2.14}$$

The initial values are given by $r(0) = r_0$ and $\phi(0) = 0$. Here, $r_0$ is the distance of closest approach. The differential equations can be solved using a fourth-order Runge–Kutta method. Another important quantity is the scattering angle, which can be obtained as

$$\Phi = \phi(t \to \infty) = \int_{r_0}^{\infty} dr \frac{2b}{r(r^2 - b^2 - r^2 V(r)/T)^{1/2}} - \pi. \tag{2.15}$$

For a given potential, the scattering angle is a function of the impact parameter $b$ and can be determined by numerical integration.

## 3. Tree-code approach to collisions

### *3.1. Collision frequency*

Pfalzner and Gibbon (1998) have studied the inverse-bremsstrahlung absorption coefficient in driven laser plasmas at moderate coupling (e.g. $\Gamma = 0.1$ and 0.5) by computer simulation techniques. Here, the non-ideality parameter is introduced as usual, $\Gamma = e^2/(4\pi\epsilon_0 a_0 k_{\mathrm{B}} T)$, and $a_0$ is the Wigner–Seitz radius $na_0^3 = 3/(4\pi)$. Using a hierarchical tree code, the heating rate of a plasma due to the action of an external field was determined. Taking the heating rate, the electron–ion collision frequency $\nu(\omega)$ was calculated as a function of the frequency at various values of the quiver velocity $v_0$, i.e. the intensity of the laser field. From this collision frequency, the emission coefficient can be obtained using the dielectric approach (cf. Bekefi (1966);

https://doi.org/10.1017/S0022377803002538 Published online by Cambridge University Press

Wierling et al. (2001))

$$j_\omega = \frac{\omega_{\rm pl}^2}{4\pi^3 c^3} k_{\rm B} T \nu(\omega). \tag{3.1}$$

Here, $\omega_{\rm pl}$ denotes the plasma frequency. We have assumed the high-frequency limit $\omega \gg \omega_{\rm pl}$. In this limit, the imaginary part of the collision frequency can be ignored and the index of refraction is unity. This relation can also be utilized to express the collision frequency in terms of the averaged Fourier-transformed force (2.1):

$$\frac{\nu(\omega)}{\omega_{\rm pl}} = \left(\frac{2\pi}{3}\right)^{3/2} (16\Gamma)^{1/2} \int_0^\infty d\bar{v}\, \bar{v}^3 e^{-\bar{v}^2} \int_0^\infty d\bar{b}\, \bar{b} |\bar{F}_{\bar{\omega}}|^2, \tag{3.2}$$

where the dimensionless quantities $\bar{\omega} = \omega \omega_{\rm pl}^{-1}$, $\bar{v} = v v_{\rm th}^{-1}$, $\bar{b} = b a_0^{-1}$ and $\bar{F} = F/(e^2/(4\pi\epsilon_0 a_0^2))$ have been introduced. $v_{\rm th}$ is the thermal velocity. As is shown in Appendix A, this result can also be obtained from an evaluation of the force–force correlation function ignoring any direct correlation among particles. However, correlations are included by assuming an effective potential of the form given in (2.6).

### *3.2. Extrapolation to the linear regime*

Making use of the heating rate in the simulation restricts the possibility of obtaining unbiased results for the collision frequency in the linear response regime. Strictly speaking, there is no heating rate within linear response. As a consequence, the smaller the intensity of the laser field, the harder it gets to distinguish the heating from thermal fluctuations. However, kinetic equation approaches including nonlinear effects (Silin 1965; Bornath et al. 2001) show a saturation of the collision frequency at small intensities. Thus, these approaches can be used to set up an extrapolation scheme in order to get the collision frequency in the linear regime from results at moderate nonlinearity. As a guideline, we use the dependence on the quiver velocity $v_0 = eE_0/m_{\rm e}\omega$ from a non-equilibrium calculation of the collision frequency in Born approximation (Bornath et al. 2001)

$$\nu(\omega) = \frac{2}{\pi^2 m_{\rm e}} \frac{n_{\rm i}}{n_{\rm e}} \sum_n \frac{n\omega}{v_0^2} \int_0^\infty dk\, k^2 V(k) \frac{{\rm Im}\epsilon_{\rm RPA}(k, n\omega)}{|\epsilon_{\rm RPA}(k, n\omega)|^2} \int_0^1 dz\, J_n^2\left(\frac{v_0 k}{\omega} z\right). \tag{3.3}$$

The quiver velocity is related to the amplitude $E_0$ of the external field, $m_{\rm e}$ is the electron mass and $\epsilon_{\rm RPA}$ the dielectric function in random phase approximation (see Kraeft et al. (1986)). $J_n$ is the Bessel function of order $n$ (Abramowitz and Stegun 1972). The index $n$ is a summation index and corresponds to the number of photons exchanged. It should be mentioned that this formula is a generalization of a result obtained by Silin (1965). Of course, it is not expected that this expression reproduces exactly the MD simulations. First of all it is a calculation only in Born approximation. Secondly, it also uses a Coulomb potential instead of the soft-core potential described above. Thirdly, it is a quantum-statistical calculation. However, it shows certain features such as the saturation at small quiver velocities. Therefore, we modified (3.3) by using the soft-core potential instead of the Coulomb potential. Next, we fit the simulation data by scaling the quiver velocity and the collision frequency itself. After these modifications, (3.3) turns out to be an efficient fit formula for the simulation results.

The method is illustrated in Fig. 1. The dynamical collision frequency obtained from simulations for various values of the quiver velocity is given at a fixed

https://doi.org/10.1017/S0022377803002538 Published online by Cambridge University Press

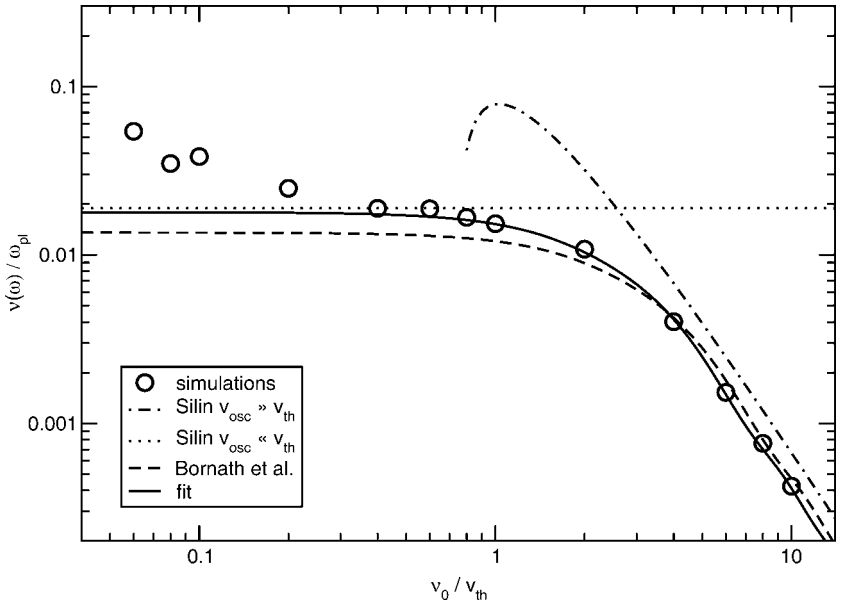



**Figure 1.** Dynamical collision frequency as a function of the quiver velocity. Non-ideality parameter $\Gamma = 0.1$. The fit function is used to extrapolate the result into the linear response region. The result in Born approximation obtained by Bornath et al. (2001) and Silin (1965) are also shown. Frequency $\omega = 5\omega_{\rm pl}$.

frequency $\omega = 5\omega_{\rm pl}$. The circles show the simulation data. The rapid increase at small quiver velocities is biased and due to thermal fluctuations. The result obtained from (3.3) is shown as well. It has the same $v_0$ dependence as the simulation data for large $v_0$. From this we fit the simulation data. The fit leads to a reasonable representation down to $v_0 = 0.4v_{\rm th}$, where $v_{\rm th}$ is the thermal velocity. The inferred collision frequency for the linear response regime is obtained by extrapolating the fit to $v_0 = 0$.

## 4. Comparison between theory and simulation

The effective potential $V^{\rm s,e}(r)$ used in our calculations is shown in Fig. 2 for $\Gamma = 0.1$ and $\epsilon = 0.2a_0$. At small distances, the effective potential stays finite, while the Coulomb as well as the Debye potential exhibit the familiar $r^{-1}$ singularity. For large distances, the potential coincides with the Debye potential. Due to the screening, the decrease is considerably stronger compared to the Coulomb potential having a $r^{-1}$ tail. The differences in the potential lead to significant changes in the scattering properties. This is illustrated in Figs. 3 and 4. The first graph shows the scattering angle as a function of the impact parameter $b$ obtained by a numerical integration of (2.15). For a Coulomb potential, the scattering angle decreases monotonically to zero with increasing $b$. For small $b$, it approaches $\pi$. Using a soft-core potential, the scattering angle for small $b$ approaches zero and a maximum arises. The account of screening leads to smaller scattering angles at large $b$, in agreement with the smaller range of the interaction due to screening. However, at small impact parameters, larger scattering angles are found. This effect can also be seen from the trajectories

https://doi.org/10.1017/S0022377803002538 Published online by Cambridge University Press

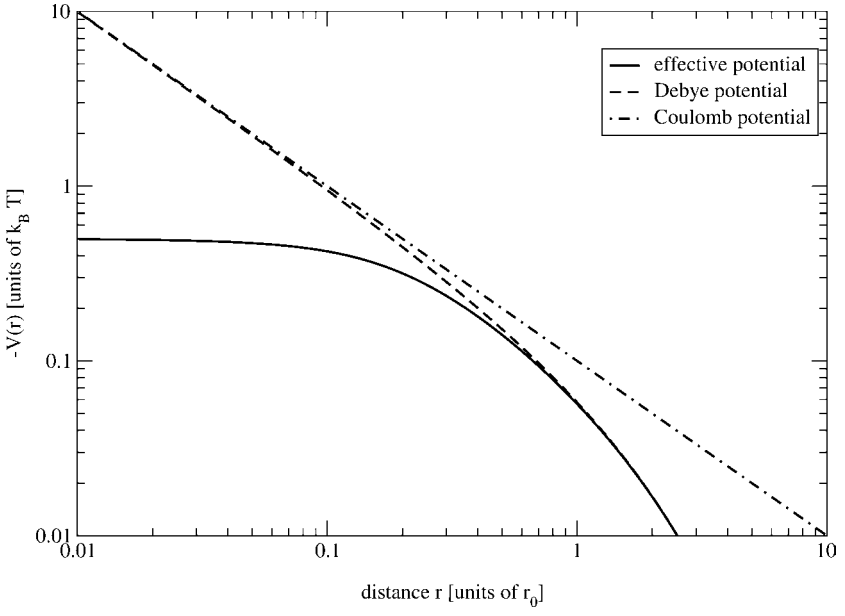



**Figure 2.** The effective potential as a function of the distance. Non-ideality parameter $\Gamma = 0.1$; softening parameter $\epsilon = 0.2a_0$. The Coulomb and the Debye potential are also compared.

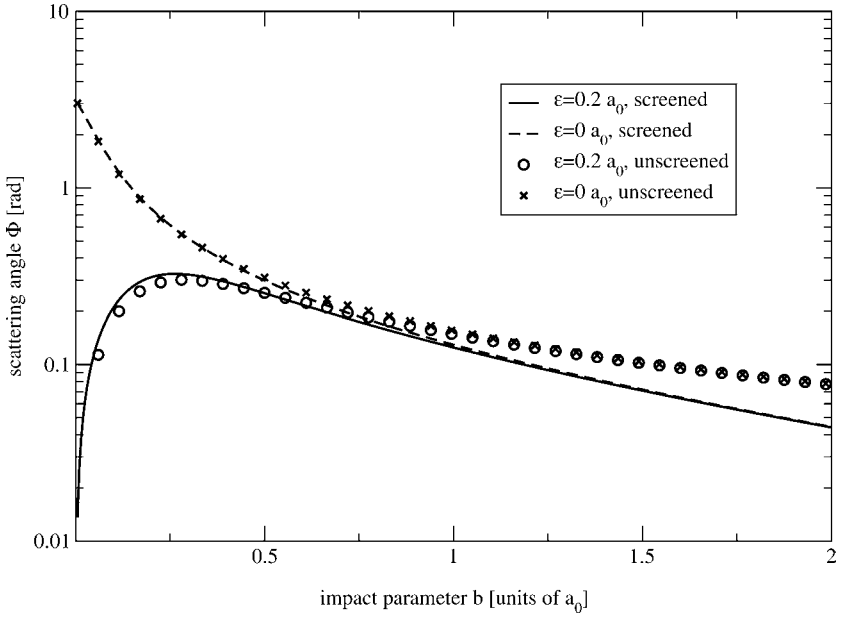



**Figure 3.** Scattering angle $\Phi$ as a function of the impact parameter $b$. Non-ideality parameter $\Gamma = 0.1$; initial velocity $v = 0.8v_{\rm th}$.

shown in Fig. 4. For $b = 0.8a_0$, the Coulomb potential leads to the largest bending of the trajectory, while the scattering is weaker for a soft-core potential, and even weaker if screening is taken into account. For $b = 0.05a_0$ and $b = 0.2a_0$, the scattering

https://doi.org/10.1017/S0022377803002538 Published online by Cambridge University Press

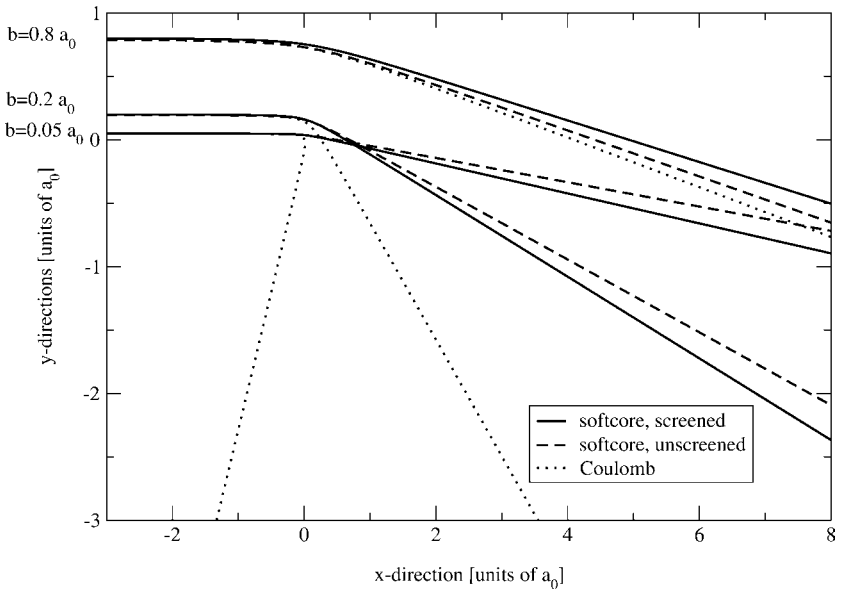



**Figure 4.** Trajectories at various impact parameters ($b = 0.05a_0$, $0.2a_0$ and $0.8a_0$) and for different potentials: Coulomb potential, unscreened soft-core potential, and screened soft-core potential. Non-ideality parameter $\Gamma = 0.1$; initial velocity $v = 0.8v_{\rm th}$.

for the soft-core potentials is also weaker compared with the Coulomb potential. The maximum of the scattering angle implies the crossing of the trajectories. However, the particle in an unscreened soft-core potential suffers the smallest effect.

Next, we determine the collision frequency according to (3.2). We calculate the trajectory from the numerical solution of the equation of motion, (2.13) and (2.15). The algorithm is tested by comparing it with the analytically known results for a Coulomb potential (see Landau and Lifshitz (1995)). From this comparison, the error in performing the integrations is estimated to be about 3–4%. The product $b|F_\omega|^2$ is shown in Fig. 5 as a function of the impact parameter $b$. The result for the effective force (2.6), the values for a Coulomb potential, a screened Coulomb potential and an unscreened soft-core potential are given. The graph for the effective force exhibits a maximum as in the case of the Coulomb potential, however at significantly higher values of $b$. As can be seen, the major effect is due to the introduction of the soft-core, while screening plays no important role for the parameters considered here.

The collision frequency $\nu(\omega)$ is shown in Fig. 6 as a function of the frequency $\omega$ for $\Gamma = 0.1$. The simulation results have been obtained employing the extrapolation scheme described above. The calculated dynamical collision frequency coincides with the simulation data within the errors. As mentioned before, the numerical integrations have an error of 3–4% which is not shown in the figure. The results for an unscreened Coulomb potential and for a SL approximation are also presented. The Coulomb results overestimate the simulation data as already expected from Fig. 5. A SL treatment on the other hand underestimates the data. A good agreement between the simulated data and the analytic approach is also found for $\Gamma = 0.5$ as is shown in Fig. 7.

https://doi.org/10.1017/S0022377803002538 Published online by Cambridge University Press

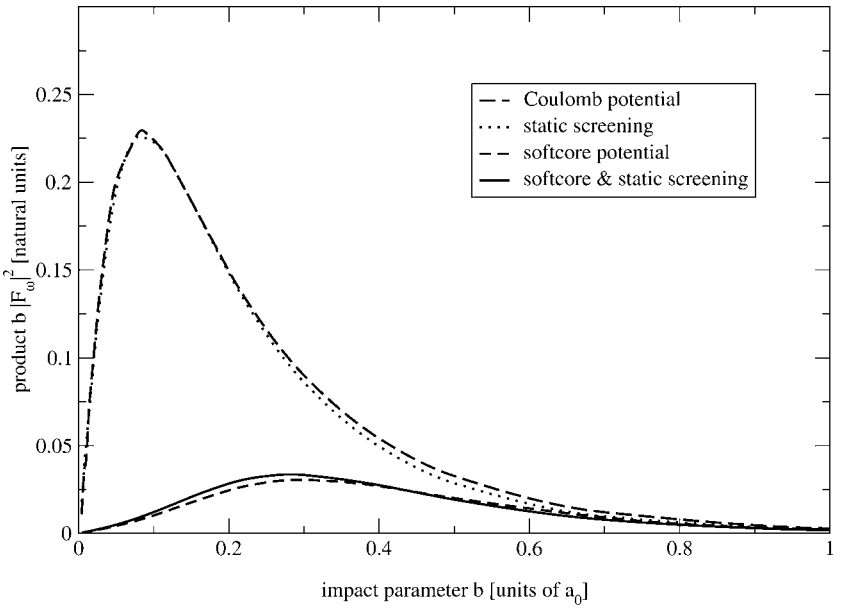



**Figure 5.** Fourier-transformed force $|F_\omega|^2$ as a function of the impact parameter $b$. The velocity is taken to be $v = 0.8 v_{\rm th}$, the frequency is $\omega = 5\omega_{\rm pl}$. Various potentials are compared.

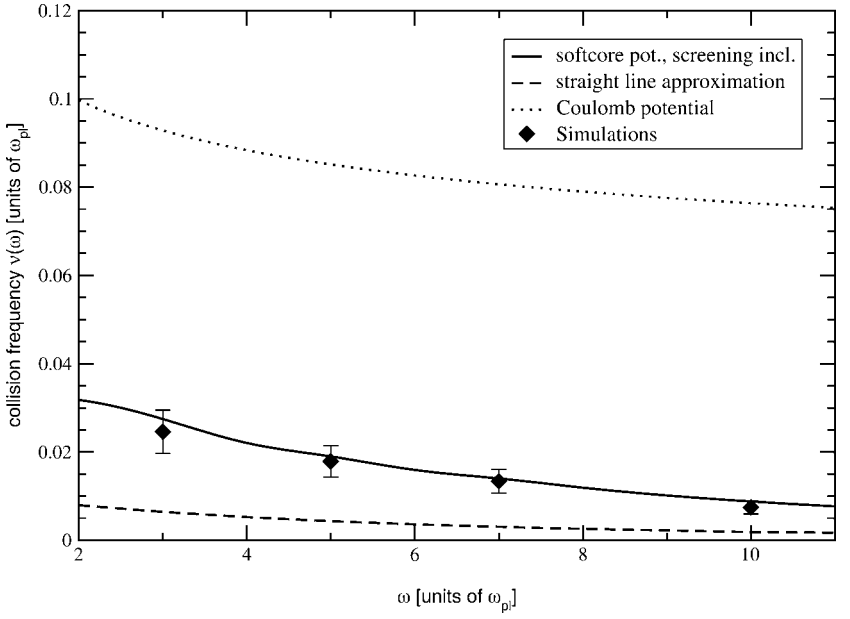



**Figure 6.** Dynamic collision frequency for $\Gamma = 0.1$ as a function of the frequency. Simulation results are compared with calculations using (3.2). The results for an unscreened Coulomb potential and for a SL approximation are shown as well.

https://doi.org/10.1017/S0022377803002538 Published online by Cambridge University Press

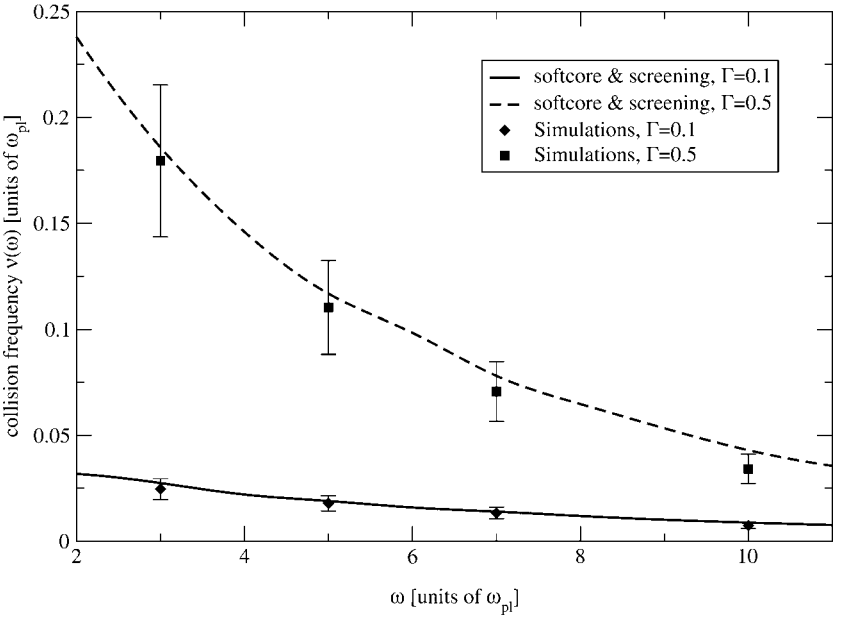



**Figure 7.** Dynamic collision frequency for $\Gamma = 0.1$ and 0.5 as a function of the frequency. Simulation results are compared with calculations using (3.2).

## 5. Conclusions

In this paper, the collision frequency in a weakly non-ideal plasma with an effective interaction was determined. The analytic results coincide within the errors with simulation data for the heating rate of the plasma due to an external field. In the dilute limit, the approach of Gould was derived from an expression for the force–force correlation function. A systematic calculation of the force–force correlation function including correlation among particles is necessary to address plasmas at moderate and strong coupling. For example, using the binary collision expansion of the Liouville operator, pair correlations in addition to collisions can be taken into account (see Sharma et al. (1997)). For a quantum mechanical system, a perturbative approach has been developed to take care of dynamical screening and collisions on the same footing (see, e.g., Reinholz et al. (2000)). Furthermore, the approach can be extended to include electron–electron collisions, which are not considered in the present paper. It is known, that electron–electron collisions have an influence on the value of the dc conductivity. These points will be investigated in a forthcoming paper.

Another closely related point needs further elaboration. A very simple product ansatz (2.6) for the effective potential including static screening has been used. Since the screening length was larger than the soft-core radius in the examples studied here, such an ansatz appears to be justified. When these scales become comparable, a detailed analysis of the screening properties of the soft-core potential has to be performed.

Yet another point is the extension to frequencies smaller than the plasma frequency. This can be achieved by going beyond the approach of Gould in using a

https://doi.org/10.1017/S0022377803002538 Published online by Cambridge University Press

generalized Drude model with the collision frequency $\nu(\omega)$. Note that the imaginary part of the collision frequency might become of importance under such conditions.

Finally, a simulation of the current–current correlation function in the long-wavelength limit would provide a direct approach to compare with our analytic approach. However, up-to-date MD simulations still have problems to achieve this limit due to restrictions on the system size.

*Acknowledgements*

We thank Dr. P. Gibbon for providing us with his tree code and Dr. H. Reinholz for stimulating discussions. AW would like to thank the Japan Society for the Promotion of Science for support under grant P02578. This paper was supported by the DFG within the SFB 198 'Kinetik partiell ionisierter Plasmen'.

## Appendix A. Classical force–force correlation function

As mentioned above, we study impurity scattering characterized by the Hamilton function

$$H(r_i, p_i, R_j) = \frac{1}{2m_\mathrm{e}} \sum_i p_i^2 + \sum_{ij} V(|\vec{r}_i - \vec{R}_j|), \tag{A 1}$$

where scattering centers are located at randomly distributed positions $R_j$, $i$ is a label running over all the electrons in the system, $m_\mathrm{e}$ is the electron mass. As was shown in Wierling et al. (2001), the collision frequency can be obtained from the Laplace transform of the force–force correlation

$$\nu(\omega) = \frac{\beta}{\epsilon_0 \omega_\mathrm{pl}^2} \langle \dot{J}_{0,z}; \dot{J}_{0,z} \rangle_{\omega+i\eta}, \tag{A 2}$$

and

$$\langle \dot{J}_{0,z}; \dot{J}_{0,z} \rangle_{\omega+i\eta} = \int_0^\infty dt e^{i(\omega+i\eta)} (\dot{J}_{0,z}(t); \dot{J}_{0,z}(0)). \tag{A 3}$$

The force–force correlation function itself is given as an ensemble average

$$(\dot{J}_{k,z}(t); \dot{J}_{k,z}(0)) = \frac{1}{Z} \int \prod_i d^3 r_i \, d^3 p_i \, d^3 R_j e^{-\beta H} \dot{J}_{k,z}(t)^* \dot{J}_{k,z}(0). \tag{A 4}$$

Classically, the electrical current is given as $\vec{J}_k = e \sum_i \vec{v}_i(t) e^{i\vec{k}\cdot\vec{r}_i(t)}$. $Z$ denotes the partition function and $H$ is the Hamilton function. In the long-wavelength limit, the time derivative of the current is given as

$$\lim_{k\to 0} \frac{dJ_{k,z}}{dt} = e \sum_i \frac{dv_{\mathrm{i},z}}{dt} = -\frac{e}{m_\mathrm{e}} \sum_i \frac{\partial H}{\partial z_i}, \tag{A 5}$$

making use of Hamilton's equation. We obtain

$$(\dot{J}_{0,z}(t); \dot{J}_{0,z}(0)) = \frac{e^2}{Z m_\mathrm{e}^2} \int \prod_i d^3 r_i \, d^3 p_i \, d^3 R_j e^{-\beta H} \sum_{ll'} \frac{\partial}{\partial z_l} \sum_j V(|\vec{r}_l(t) - \vec{R}_j|)$$

$$\times \frac{\partial}{\partial z_{l'}} \sum_{j'} V(|\vec{r}_{l'}(0) - \vec{R}_{j'}|). \tag{A 6}$$

https://doi.org/10.1017/S0022377803002538 Published online by Cambridge University Press

In the low density limit, the collisions are well separated in time. Furthermore, correlations among the particles can be neglected. We obtain

$$(\dot{J}_{0,z}(t);\dot{J}_{0,z}(0)) = \frac{n_e n_i e^2}{3m_e^2}\left(\frac{1}{2\pi m_e k_B T}\right)^{3/2}\int d^3r\, d^3p e^{-\beta p^2/(2m_e)}\vec{F}(|\vec{r}(t)|)\cdot\vec{F}(|\vec{r}(0)|), \quad (A\,7)$$

Each of the particles moves on a trajectory, which can be characterized uniquely by an energy $E$ and an impact parameter $b$. Thus, the integral over the position is converted as $\int d^3x \to \int b\,db\int_{-\infty}^{\infty} dt'$. Utilizing the low density limit, we arrive at

$$\int_0^\infty dt e^{i\omega t}\int d^3r\,\vec{F}(\vec{r}(t))\cdot\vec{F}(\vec{r}(0)) = \int_0^\infty db\, b|\vec{F}_\omega|^2 \quad (A\,8)$$

making use of the Wiener–Khinchin theorem. By introducing dimensionless variables, we arrive at expression (3.2).

## References


Griem, H. R. 1997 *Principles of Plasma Spectroscopy*. Cambridge: Cambridge University Press.

Hutchinson, I. H. 1987 *Principles of Plasma Diagnostics*. Cambridge: Cambridge University Press.

Voss, K. E. and Fisch, N. J. 1992 Inverse problem for bremsstrahlung radiation. *Phys. Fluids B* **4**, 762–763.

Voss, K. E. and Fisch, N. J. 1993 *Phys. Fluids B* **5**, 659(E).

Bekefi, G. 1966 *Radiation Processes in Plasmas*. New York: Wiley.

Sobelman, I. I. 1992 *Atomic Spectra and Radiation Transitions*. Berlin: Springer.

Jackson, J. D. 1999 *Classical Electrodynamics*, 3rd edn. New York: Wiley.

Dawson, J. M. and Oberman, C. 1962 High-frequency conductivity and the emission and Absorption coefficient of a fully ionized plasmas. *Phys. Fluids* **5**, 517–524.

Berkovsky, M. and Kurilenkov, Y. K. 1993 Electron dynamic correlations in strongly coupled plasmas: beyond the Born approximation. *Physica A* **197**, 676–695.

Cauble, R. and Rozmus, W. 1985 Inverse bremsstrahlung absorption coefficient in collisional plasmas. *Phys. Fluids* **28**, 3387–3392.

Kawakami, R., Mima K., Totsuji, H. and Yokoyama, Y. 1988 Bremsstrahlung from hot, dense, partially ionized plasmas. *Phys. Rev. A* **38**, 3618–3627.

Silin, V. P. Nonlinear high-frequency plasma conductivity. *Sov. Phys. JETP* **20**, 1510–1516.

Decker, C. D., Mori, W. B., Dawson, J. M. and Katsouleas, T. 1994 Nonlinear collisional absorption in laser-driven plasmas. *Phys. Plasmas* **1**, 4043–4049.

Bornath, Th., Schlanges, M., Hilse, P. and Kremp, D. 2001 Nonlinear collisional absorption in dense laser plasmas. *Phys. Rev. E* **64**, 026414.

Wierling, A., Millat, Th., Röpke, G., Redmer, R. and Reinholz, H. 2001 Inverse bremsstrahlung of hot, weakly coupled plasmas. *Phys. Plasmas* **8**, 3810–3819.

Gould, R. J. 1970 Low-frequency Bremsstrahlung in coulomb scatterings of nonrelativistic electrons. *Am. J. Phys.* **38**, 189–201.

Jung, Y.-D. 1994 Thermal and nonthermal electron–ion bremsstrahlung spectrum from high-temperature plasmas. *Phys. Plasmas* **1**, 785–788.

Jung, Y.-D. 1996 Plasma-screening effects on bremsstrahlung in electron–ion Coulomb scatterings in strongly coupled plasmas. *Phys. Plasmas* **3**, 1741–1744.


https://doi.org/10.1017/S0022377803002538 Published online by Cambridge University Press

Jung, Y.-D. and Jeong, H.-D. 1996 Bremsstrahlung in electron–ion Coulomb scattering in strongly coupled plasma using the hyperbolic-orbit trajectory method. *Phys. Rev. E* **54**, 1912–1917.

Jung, Y.-D. 2002 Classical bremsstrahlung radiation from electron–ion encounters in a nonideal plasma. *J. Plasma Phys.* **67**, 191–197.

Kim, Longhuan and Pratt, R. H. 1987 Numerical calculation of classical bremsstrahlung *Phys. Rev. A* **36**, 45–58.

Kraeft, W.-D., Kremp, D., Ebeling, W. and Röpke, G. 1986 *Quantum Statistics of Charged Particle Systems*. New York: Plenum.

Jung, Y.-D. 1997 Dynamic screening effects on electron–ion Coulomb bremsstrahlung in dense plasmas. *Phys. Rev. E* **55**, 3369–3372.

Landau, L. D. and Lifshitz, E. M. 1995 *The Classical Theory of Fields*, 4th edn. Oxford: Pergamon.

Abramowitz, M. and Stegun, I. 1972 *Handbook of Mathematical Functions*. New York: Dover.

Kelbg, G. 1963 Theorie des Quanten-Plasmas. *Ann. Phys. (Leipzig)* **12**, 219–224.

Deutsch, C. 1977 Nodal expansion in a real matter plasma. *Phys. Lett. A* **60**, 317–318.

Pfalzner, S. and Gibbon, P. 1998 Direct calculation of inverse-bremsstrahlung absorption in strongly coupled, nonlinear driven laser plasmas. *Phys. Rev. E* **57**, 4698–4705.

Sharma, R. K., Tankeshwar, K., Pathak, K. N., Ranganathan, S. and Johnson, R. E. 1997 Binary collision contribution to the longitudinal current correlation function of dense fluids. *Phys. Rev. E* **55**, 1550–1557.

Reinholz, H., Redmer, R., Röpke, G. and Wierling, A. 2000 Long-wavelength limit of the dynamical local-field factor and dynamical conductivity of a two-component plasma. *Phys. Rev. E* **62**, 5648–5666.

https://doi.org/10.1017/S0022377803002538 Published online by Cambridge University Press